Journal of the American College of Cardiology
© 2001 by the American College of Cardiology
Published by Elsevier Science Inc.

Vol. 38, No. 3, 2001
ISSN 0735-1097/01/$20.00
PII S0735-1097(01)01466-8

Attenuation of Interatrial Conduction Using Right Atrial Septal Catheter Ablation

David Schwartzman, MD, FACC,* Eduardo N. Warman, PHD,† William A. Devine, BS,‡ Rahul Mehra, PHD†

Pittsburgh, Pennsylvania and Minneapolis, Minnesota

OBJECTIVES We sought to characterize a method of attenuating interatrial conduction using radiofrequency ablated lesions applied to the right atrial septum.

BACKGROUND Interatrial conduction occurs in specific zones. Recent data suggest that interatrial conduction can be important in triggering and sustaining atrial fibrillation. Therefore, a method for attenuating interatrial conduction may have therapeutic value.

METHODS In 13 healthy pigs, interatrial conduction was evaluated before and after sequential ablation of the right atrial septum, targeting interatrial conduction zones. In six animals, zone 1 (crista terminalis and limbus) was ablated first, followed by ablation of zone 2 (fossa ovalis and coronary sinus ostium). In the other seven animals, the order of ablation was reversed. Electrophysiologic and pathologic findings were correlated.

RESULTS After ablation of zone 1, interatrial conduction was slowed, but there was no block. After ablation of zone 2, conduction was unchanged. After ablation of both zones, complete block was observed in four animals, and there was left atrial quiescence. In the remaining nine animals, incomplete block was observed, with marked conduction slowing or block during sinus rhythm and pacing. Ablation did not adversely affect atrioventricular node conduction, nor did it facilitate sustenance of an atrial arrhythmia. Pathologic analysis revealed that complete interatrial conduction block was associated with confluent ablation of both targeted zones.

CONCLUSIONS Catheter ablation of the right atrial septum attenuated interatrial conduction without disturbing atrioventricular conduction. (J Am Coll Cardiol 2001;38:892–9) © 2001 by the American College of Cardiology

The anatomy of the interatrial septum has been the subject of several reports, some of which have included descriptions of interatrial myocardial connections (1–9). Distinct zones of interatrial conduction have been correlated with these connections (10–12). Previous reports have suggested that intact interatrial conduction is important for triggering and sustaining atrial fibrillation (AF) (13–16). Thus, it has been hypothesized that attenuation of interatrial conduction might have therapeutic utility. A surgical method for eliminating interatrial conduction has been reported, and this method has resulted in a reduction in the incidence of AF (17). However, this method employed a continuous, transmural left atrial incision that leaves the septum intact. In addition, sternotomy and cardiopulmonary bypass were necessary.

The present study is based on the hypothesis that significant attenuation, including complete block, of interatrial conduction could be achieved using percutaneous radiofrequency catheter ablation to target right atrial septal endocardial sites that are associated with interatrial myocardial connections.

From the *Atrial Arrhythmia Center, University of Pittsburgh, Pittsburgh, Pennsylvania; †Medtronic, Inc., Minneapolis, Minnesota; and ‡Department of Pathology, Children's Hospital of Pittsburgh, Pittsburgh, Pennsylvania. This study was supported in part by a grant from Medtronic, Inc., Minneapolis, Minnesota.

Manuscript received July 6, 2000; revised manuscript received May 21, 2001, accepted June 4, 2001.

METHODS

Animal model. Thirteen large (35 to 60 kg) healthy Hanford pigs were used. It has been previously demonstrated that atrial anatomy in this animal is similar to that of humans (18). After endotracheal intubation, a surgical plane of anesthesia was maintained using 1% to 4% isoflurane. Arterial blood was was monitored throughout the procedure. Access to the right atrium was achieved percutaneously through the femoral vein. Access to the left atrium was achieved through the femoral vein and atrial septal puncture.

Imaging. Two nonfluoroscopic techniques were used: 1) this CARTO (Biosense/Webster, Diamond Bar, California) system employs synchronous extracorporeal magnetic fields to determine the location and orientation of a sensor mounted within an intracardiac catheter (NaviStar, Biosense/Webster) near its distal electrode (19). 2) Intracardiac echocardiography (ICE). The system was composed of a 9F catheter (Boston Scientific, Natick, Massachusetts) incorporating a rotating transducer operating at 9 MHz (20). The catheter was placed into the right atrium. Intracardiac echocardiography provided a detailed image of each of the right atrial septal anatomic landmarks (21).

Electrophysiologic study. In addition to the NaviStar and ICE catheters, standard quadripolar catheters were placed in the right atrial appendage (RAA) and left atrial appendage (LAA). These catheters were positioned at the beginning of the experiment and remained in place for its

Abbreviations and Acronyms

AF = atrial fibrillation
AVN = atrioventricular node
Δ_{max} = maximal difference between interatrial conduction times during atrial extrastimulation
ERP = local atrial effective refractory period
ICE = intracardiac echocardiography
ICT = interatrial conduction time, measured by interval between RAA and LAA
LAA = left atrial appendage
P_{Dur} = maximal duration of surface P wave, derived from 12-lead electrocardiogram
RAA = right atrial appendage
SCL = sinus cycle length

duration. The distal electrode pairs of each catheter were used for pacing, and the proximal pair for measurement of activation times. At baseline, an electrophysiologic study was performed, consisting of several indexes: 1) Sinus rhythm: sinus cycle length (SCL), corrected sinus node recovery time, maximal duration of surface P-wave, derived from the 12-lead electrocardiogram (P_{Dur}), PQ interval (P-wave onset to QRS onset), interval between local activation of the right atrial appendage and local activation of the atrium adjacent to this His bundle (RAA-HB_A) and interatrial conduction time, measured by interval between RAA and LAA (ICT). 2) RAA pacing: atrioventricular node (AVN) Wenckebach cycle length, ICT at a pacing cycle length of 500 ms (ICT_{500}; pacing was also performed at cycle lengths of 400, 350, 300, 250 and 200 ms; observations at these cycle lengths are reported, but ICTs are not), AVN local atrial effective refractory period (ERP), ICT during extrastimulation (500 ms drive cycle), with coupling intervals between 400 ms and ERP (10 ms steps), and ERP. Inducibility of atrial tachyarrhythmia was evaluated with RAA burst pacing (20 mA, 2 ms pulse width) at a cycle length of 100 ms for 10 s. 3) LAA pacing: same as RAA pacing.

Because of differences in the exact positions of the RAA and LAA electrodes between animals, baseline ICT varied. To combine individual data to assess the relationship between ICT and the atrial extrastimulus coupling interval, conduction times in each animal were expressed as the difference (Δ) from the ICT measured at the longest extrastimulus coupling interval (400 ms). The maximal difference between interatrial conduction times during atrial extrastimulation (Δ_{max}) for each extrastimulation procedure was measured.

Ablation technique. The NaviStar catheter was used for radiofrequency energy applications. This catheter is 7F with a 4.5-mm length distal ablation electrode, with a thermocouple embedded near its tip. Radiofrequency energy was applied in unipolar fashion to the right atrial septum. Energy titration was guided by electrode thermometry, with a target ablation temperature of 60°C for 60 s. Intracardiac echocardiography (ICE) and the CARTO system were utilized in tandem: ICE was utilized to define right atrial septal anatomy, to position the ablation electrode relative to anatomic structures and to ensure firm, stable electrode-endocardial contact during each radiofrequency application; CARTO was used to record lesion locations. For purposes of guiding ablation, four anatomic areas were grouped into two "zones": zone 1 (crista terminalis and limbus) and zone 2 (fossa ovalis and coronary sinus ostium) (Fig. 1). Ablation of each zone was performed using a series of radiofrequency applications. Each radiofrequency application site was demarcated by CARTO as a spherical icon with a diameter of 4 mm (19). Ablation of a septal zone was defined as complete when icons filled the zone and no significant near-field potentials could be recorded within the zone.

Pathology. Animals were sacrificed immediately. The atria were removed en bloc and immersed in a bath of 1% triphenyl tetrazolium chloride for 60 min. The specimens were photographed within 24 h of death. Endocardial lesion dimensions were measured using photographic planimetry.

Experimental protocol. After the baseline electrophysiologic study, ablation was performed. In six animals, zone 1 was ablated first; in seven animals, zone 2 was ablated first. The first ablation zone was chosen at random. The electrophysiologic study was repeated after ablation of each zone.

Analytical methods. Data are reported as the mean value ± SD, unless otherwise specified. Baseline and post-ablation data were compared by analysis of variance, with use of the Bonferroni test for multiple comparisons. A p value <0.05 was considered statistically significant.

Definitions. *Complete interatrial conduction block*—no interatrial conduction during sinus rhythm or atrial pacing at any cycle length. *Atrial fibrillation*—tachycardic atrial electrogram varying in cycle length and morphology; defined as "transient" if it persisted for ≥5 s but terminated spontaneously within 60 s. *Atrial flutter*—tachycardiac atrial electrogram with constant cycle length and morphology; defined as "transient" if it persisted for ≥5 s but terminated spontaneously within 60 s. *Atrial tachyarrhythmia* (AF, flutter) inducibility—tachyarrhythmia observed after ≥50% of induction attempts.

RESULTS

Electrophysiologic study (Table 1). BASELINE. Interatrial conduction block was not observed during sinus rhythm or pacing. Interatrial conduction times in either direction were similar. The ERP in the LAA was significantly shorter than that in the RAA. Left atrial extrastimulation was associated with a significantly larger Δ_{max} relative to right atrial extrastimulation. However, at extrastimulus coupling intervals that could be tested in both atria (e.g., >RAA ERP), there was no significant difference. Transient "bi-atrial" AF (e.g., AF in both RAA and LAA electrograms) was inducible in each animal from the LAA and RAA. No atrial flutter was induced.

JACC Vol. 38, No. 3, 2001
September 2001:892–9

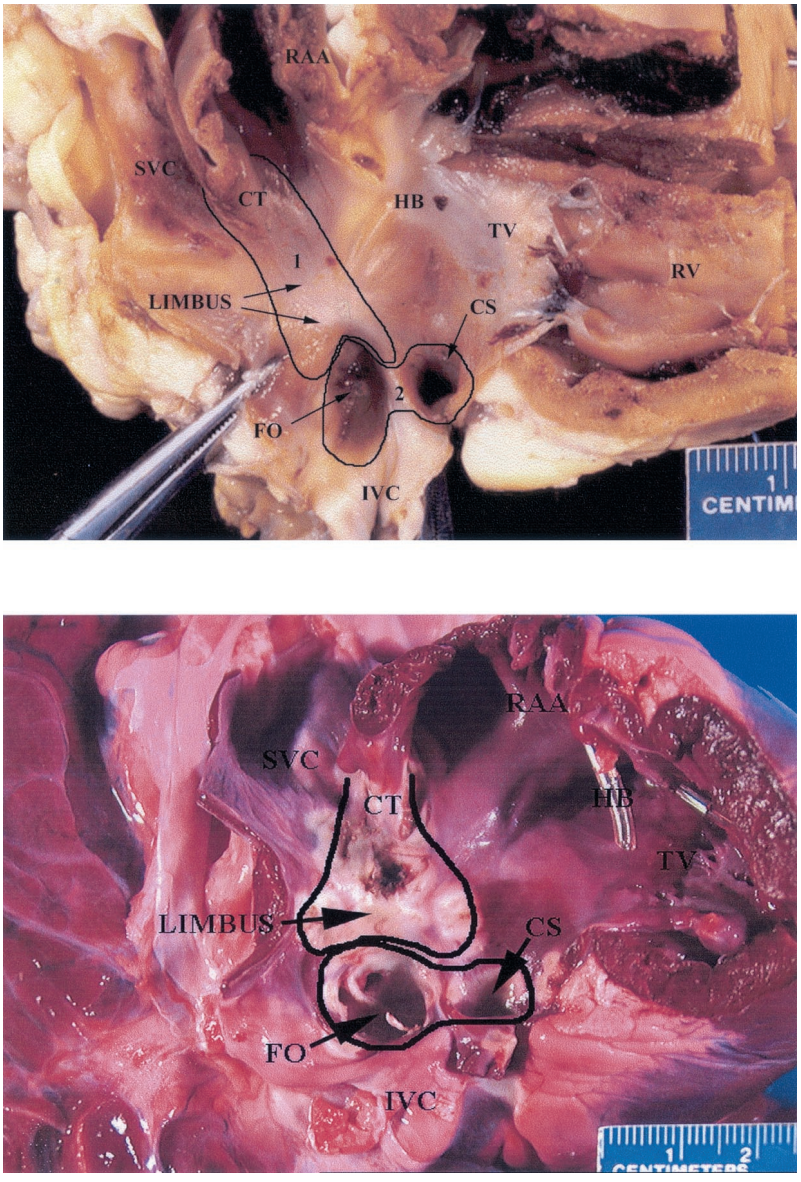

Figure 1. Endocardial view of right atrial septum. **(Top)** Healthy heart specimen. The territories encompassed by zones 1 and 2 are encircled. CS = coronary sinus ostium; CT = medial (septal) portion of crista terminalis; FO = oval fossa; HB = region of His bundle (apex of Koch's triangle); IVC = inferior vena cava; RAA = medial wall of right atrial appendage; RV = septal wall of right ventricular inflow tract; SVC = superior caval vein; TV = septal leaflet of tricuspid valve. **(Bottom)** Postablation specimen. This subject had complete interatrial conduction block. The specimen was stained with triphenyl tetrazolium chloride, rendering "viable" myocardium deep red and ablated myocardium white.

AFTER ABLATION OF ZONE 1 (CRISTA TERMINALIS AND LIMBUS) FIRST. The P-wave duration and right intra-atrial conduction time were both significantly increased relative to baseline (Fig. 2). There was also a significant increase in the interatrial conduction time during both sinus rhythm and pacing, but no conduction block. There were no significant differences in Δ_{max} values relative to baseline. Transient bi-atrial AF was inducible in each animal from the LAA and RAA. No atrial flutter was induced.

AFTER ABLATION OF ZONE 2 (FOSSA OVALIS AND CORONARY SINUS OSTIUM) FIRST. No significant changes were noted in the P-wave duration, right intra-atrial conduction time or interatrial conduction time. There was no interatrial conduction block. There were no significant differences in Δ_{max} values relative to baseline. Transient bi-atrial AF was inducible in each animal from the LAA and RAA. No atrial flutter was induced.

AFTER ABLATION OF BOTH ZONES. During sinus rhythm, four animals had complete interatrial conduction block, and nine animals had incomplete block.

1) Complete interatrial conduction block: despite a marked increase in the right intra-atrial conduction time, the P-wave duration was significantly decreased due to loss of the left atrial component (Fig. 2). There was no intrinsic left atrial rhythm (Fig. 3). There was no significant change in AVN conduction. During RAA stimulation, neither AF

Table 1. Summary Data from Before Ablation (Baseline) and Ablation of Zone 1 First, Zone 2 First and Zones 1 and 2 (Separated Into Whether Incomplete or Complete Interatrial Conduction Block Was Observed After All Ablation Lesions Were Deployed)

				Zones 1 and 2	
	Baseline	**Zone 1**	**Zone 2**	**Incomplete**	**Complete**
Subjects (n)	13	6	7	9	4
RF applications	—	23–42	29–44	52–83	46–79
Sinus rhythm					
SCL	706 ± 73	**553 ± 50**	685 ± 87	**538 ± 33**	**555 ± 66**
CSNRT	102 ± 83	168 ± 59	153 ± 39	93 ± 44	104 ± 11
P_{Dur}	70 ± 10	**117 ± 17**	70 ± 11	**137 ± 24**	**51 ± 11**
PR	129 ± 21	**158 ± 23**	121 ± 15	**158 ± 15**	**184 ± 41**
RAA-HB_A	120 ± 12	**145 ± 6**	115 ± 21	**151 ± 15**	**173 ± 52**
ICT	25 ± 17	**72 ± 19**	14 ± 11	**111 ± 29***	—
ICB (n)	0	0	0	2	4
RAA pacing					
ERP	199 ± 28	178 ± 38	205 ± 13	184 ± 13	183 ± 31
AVN WCL	294 ± 45	278 ± 61	263 ± 25	303 ± 79	268 ± 39
AVN ERP	316 ± 24	304 ± 34	300 ± 23	**267 ± 23**	280 ± 10
ICT_{500}	63 ± 13	**94 ± 30**	63 ± 13	**121 ± 39**	
ICB_{pace} (n)	0	0	0	5†	4
Δ_{max}	9 ± 2	16 ± 12	18 ± 10	**118 ± 36**‡	—
$ICB_{extrastim}$ (n)	0	0	0	2‡	—
AFCL-RAA	176 ± 47	169 ± 33	181 ± 23	185 ± 57	NI
AFCL-LAA	169 ± 32	154 ± 41	162 ± 55	232 ± 104	NI
LAA pacing					
ERP	158 ± 22	140 ± 19	160 ± 8	142 ± 16	155 ± 135
AVN WCL	285 ± 71	248 ± 39	263 ± 75	267 ± 41	350, 400
AVN ERP	315 ± 28	300 ± 37	295 ± 42	**270 ± 33**	280#
ICT_{500}	69 ± 18	**91 ± 36**	60 ± 6	**101 ± 24**§	—
ICB_{pace} (n)	0	0	0	3‖	4
Δ_{max}	39 ± 22	32 ± 5	45 ± 13	**92 ± 41**¶	—
$ICB_{extrastim}$ (n)	0	0	0	3¶	—
AFCL-RAA	166 ± 51	181 ± 42	177 ± 41	**315 ± 43**	NI**
AFCL-LAA	152 ± 30	155 ± 25	149 ± 39	157 ± 24	145 ± 53

Data in bold indicate $p < 0.05$ versus baseline value, utilizing paired data only (e.g., the paired *t* test between baseline and zone 1 sinus cycle length was based on only the six animals that had zone 1 ablated first and their six paired pre-ablation values). All values are in ms (mean ± SD), except for: 1) entities demarcated by (n), referring to the number of subjects, and 2) radiofrequency energy applications, given as the range of applications in the cohort. *Data from the seven subjects with intact interatrial conduction. †In three animals, block manifested Wenckebach periodicity. Pacing cycle lengths at which block was observed (n = 5): all (n = 2), 400 ms (n = 1), 300 ms (n = 1), and 200 (n = 1). ‡Data from the seven subjects with intact interatrial conduction at the drive cycle length of 500 ms. §Data from the eight subjects with intact interatrial conduction. ‖In two animals, block manifested Wenckebach periodicity. Pacing cycle lengths at which interatrial conduction block was observed (n = 3): all (n = 1), 300 ms (n = 1) and 200 ms (n = 1). Note that the animal in which block was observed at all pacing cycle lengths was *not* one of the two animals in which block was observed during sinus rhythm. Each of those animals had intact interatrial conduction during LAA pacing at 500 ms, with block occurring at 300- and 200-ms pacing cycle lengths, respectively. ¶Data from eight subjects with intact interatrial conduction during the drive cycle length of 500 ms. #Data available in only one of the two animals in which left atrioventricular conduction was demonstrated. **Right atrium in sinus rhythm.

AFCL = atrial fibrillation cycle length; AVN = atrioventricular node; CSNRT = corrected sinus node recovery time; ERP = effective refractory period; ICB = interatrial conduction block; $ICB_{extrastim}$ = interatrial conduction block during extrastimulation; ICB_{pace} = interatrial conduction block during pacing at a fixed cycle length; ICT = interatrial conduction time; ICT_{500} = electrical conduction time at an atrial pacing cycle length of 500 ms; LAA = left atrial appendage; NI = atrial fibrillation not inducible; P_{Dur} = maximal duration of surface P wave; RAA = right atrial appendage; RAA-HB_A = interval between local activation of the right atrial appendage and local activation of the atrium adjacent to the His bundle; SCL = sinus cycle length; WCL = Wenckebach cycle length; Δ_{max} = maximal difference between interatrial conduction times during atrial extrastimulation.

nor flutter was inducible in any animal. During LAA stimulation, only transient left atrial AF was inducible in each animal; the right atrium remained in sinus rhythm (Fig. 4).

Left atrioventricular block, defined by ventricular activation at the SCL despite left atrial pacing at a sub-SCL, was observed in two animals. In the other two animals, intact left atrioventricular conduction was observed. In each case, the electrocardiographic QRS morphology was identical to that in sinus rhythm. In the first animal, the LAA-QRS interval during pacing at 500 ms was 260 ms, whereas the RAA-QRS interval during pacing at 500 ms was 150 ms. Left atrioventricular block occurred in a Wenckebach pattern at a cycle length of 350 ms (right atrioventricular block cycle length of 240 ms). In the second animal, the LAA-QRS interval during pacing at 500 ms was 390 ms, whereas the RAA-QRS interval during pacing at 500 ms was 180 ms. Left atrioventricular block occurred in a Wenckebach pattern at 400 ms (right atrioventricular block cycle length of 300 ms).

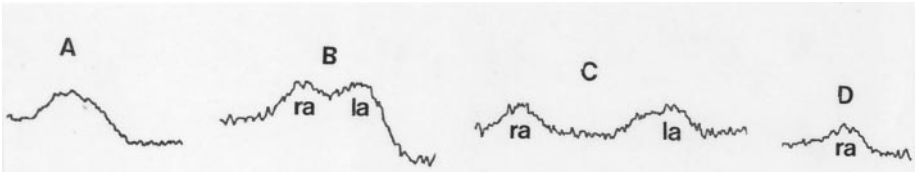

Figure 2. Typical surface P waves at baseline **(A),** after zone 1 ablation **(B),** after ablation of zones 1 and 2 with incomplete interatrial conduction block **(C)** and after ablation of zones 1 and 2 with incomplete interatrial conduction block **(D).** ra = component of P-wave associated with right atrial activation; la = component of P-wave associated with left atrial activation.

2) Incomplete interatrial conduction block: during sinus rhythm, block was observed in two animals. In both of these animals, interatrial conduction was intact during left atrial pacing at cycle lengths similar to those in sinus rhythm. In the other seven animals, interatrial conduction was intact during sinus rhythm, albeit with a markedly prolonged duration. This was associated with a marked increase in the P-wave duration, with the emergence of two discrete complexes (Fig. 2).

During right atrial pacing, block was observed at all pacing cycle lengths in the two animals with block in sinus rhythm. Block was observed in three additional animals at cycle lengths ranging from 400 to 200 ms; in each of these animals, block had a Wenckebach periodicity. During extrastimulation in the seven animals with intact conduction at the drive cycle length, Δ_{max} was significantly increased. Block was observed in two of the seven animals. Transient AF, with a mean LAA cycle length significantly longer than the mean RAA cycle length, was inducible in four of the nine animals. No atrial flutter was induced in any animal.

During left atrial pacing in the two animals exhibiting block in sinus rhythm, intact interatrial conduction was observed at a cycle length of 500 ms. In another animal, block was demonstrated at all cycle lengths, despite intact interatrial conduction in sinus rhythm. Block was observed in two additional animals at cycle lengths ranging from 300 to 200 ms; in each animal, block had a Wenckebach periodicity. During extrastimulation in the eight animals with intact conduction at the drive cycle length, Δ_{max} was significantly increased. Block was observed in three of the eight animals. Transient AF, with a mean RAA cycle length

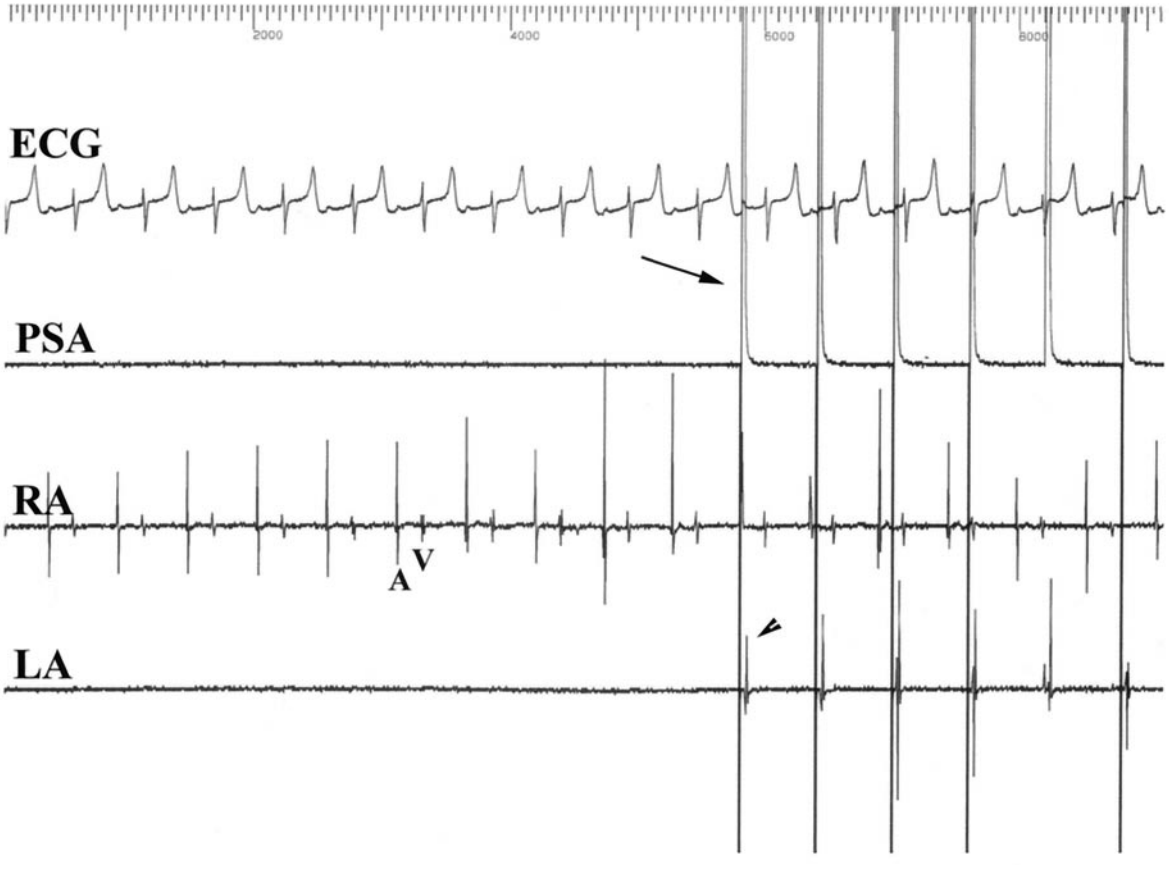

Figure 3. Surface electrocardiographic, left atrial appendage (LAA) pacing stimulus artifact (PSA) and right atrial (RA) and left atrial (LA) recordings after complete interatrial conduction block. In the left half of the figure, there is no pacing. The left atrium is electrically quiescent. In the right half of the figure, LAA pacing **(arrow)** demonstrates left atrial capture **(arrowhead),** which is dissociated from the right atrium.

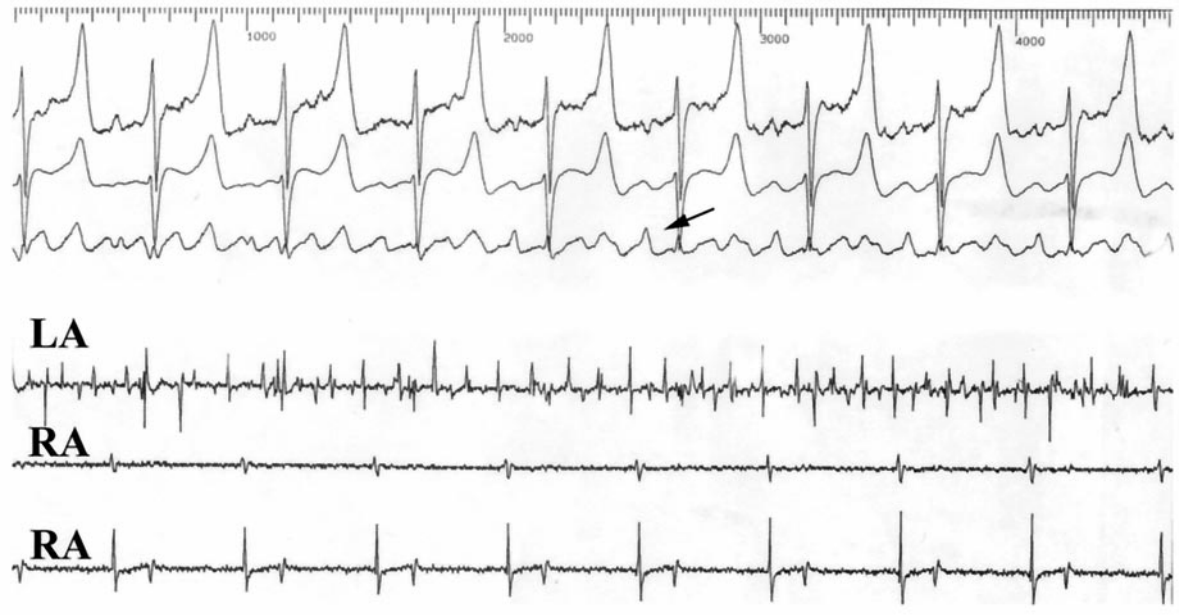

Figure 4. Three surface electrocardiographic, one left atrial (LA) and two right atrial (RA) intracardiac recordings are shown during atrial fibrillation, which was induced after complete interatrial conduction block by left atrial appendage burst pacing. The right atrium is in sinus rhythm. The surface electrocardiogram manifests a "hybrid" morphology composed of both regular **(arrow)** and fibrillatory activity.

longer than the mean LAA cycle length, was inducible in all animals (Fig. 5). No atrial flutter was induced in any animal.

In the animals with incomplete block and intact left-to-right interatrial conduction, ICE-guided CARTO activation mapping of the right atrium was performed during LAA pacing (550 ms cycle length) (19). In each animal, the chamber was activated by a single wave front entering the right atrium through the coronary sinus ostium.

Pathology. The area of the zone 1 ablation lesion was 1.7 ± 0.6 cm^2 and that of zone 2 was 1.4 ± 0.4 cm^2 (Fig. 1). There was no damage to the triangle of Koch. The left atrial septum had minimal lesions limited to the area opposite the fossa ovalis. In animals with complete block, the ablation lesion was confluent in each zone. In each of the animals with incomplete block, one or more lesion gaps in the coronary sinus ostium, ranging in total area from 2 to 18 mm^2, were observed.

DISCUSSION

Interatrial conduction. Our data indicate that ablation of the right atrial septum, targeting anatomic areas associated with interatrial myocardial connections, results in attenuation of interatrial conduction, including complete interatrial conduction block. This was associated with preserved sinus node and AVN function.

After ablation of zone 1 but not zone 2, both the sinus P-wave duration and interatrial conduction times were significantly increased relative to baseline. After ablation of either zone, the response of interatrial conduction during pacing or extrastimulation was similar to that at baseline. These data suggest that, based on the proximity to the sinus node, zone 1 connections were primarily responsible for the P-wave duration. The superior locations of both the RAA and LAA recording catheters explain the correlation between the sinus P-wave duration and interatrial conduction time. These data demonstrate the limited utility of the P-wave duration for assessing overall interatrial conduction properties.

After ablation of both zones 1 and 2, interatrial conduction times increased dramatically, and decremental properties were observed. In some animals, complete bi-directional conduction block was observed. In other animals, block was incomplete, occurring uni-directionally or at sub-SCL, or both. In animals with incomplete conduction block, interatrial conduction times were longer than those after zone-1 ablation alone, indicating that ablation of zone 2 added to conduction slowing.

Atrial tachyarrhythmia inducibility. Inducibility of atrial tachyarrhythmias before and after ablation was limited to transient AF. These data suggest that the lesions deployed in the present study did not promote sustenance of fibrillation or flutter. In fact, our observations of left atrial quiescence (Fig. 3), right atrial sinus rhythm during left AF (Fig. 4) asymmetric AF cycle length (Fig. 5) are similar to those reported after surgical left or right atrial isolation or the Corridor procedure, or both (22,23).

Left atrioventricular conduction. In animals with complete conduction block, no intrinsic electrical activity of the left atrium was observed. Quiescence has also been reported after the surgical isolation procedure in humans (17). Complete interatrial conduction block afforded a unique opportunity to probe for left atrioventricular conduction. In two of four animals, such conduction was observed. Relative to sinus rhythm and right atrial pacing, the atrioventricular

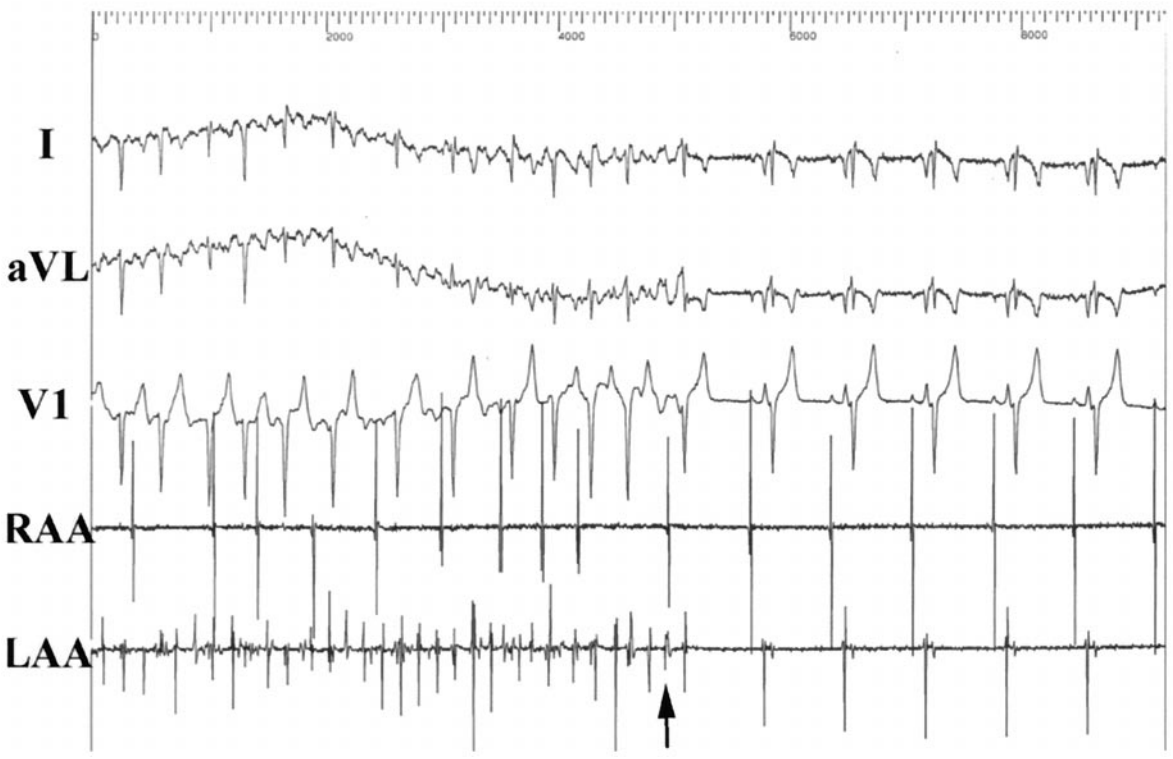

Figure 5. Left atrial fibrillation, induced by left atrial appendage (LAA) burst pacing. Note that during electrocardiographic atrial fibrillation (AF), the right atrial activation rate is markedly less than the left atrial activation rate. The AF terminates **(arrow),** after which interatrial conduction is intact. Note also that the ventricular activation rate is significantly faster than the right atrial activation rate, consistent with activation of the atrioventricular node by a route other than the right atrium. RAA = right atrial appendage.

conduction time during left atrial pacing was markedly prolonged, and atrioventricular block occurred with Wenckebach periodicity. Although inconclusive, these data suggest that there are inputs to the AVN from the left atrium that may be independent of, and less robust than, right atrial inputs in this animal model.

Pathology. In the present study, confluent ablation of both zones was necessary to achieve complete interatrial conduction block. Incomplete block was consistently associated with one or more lesion gaps, always in the coronary sinus ostium. Lesion gaps limited to the same area in all animals suggest a systematic fault in the ablation procedure, possibly associated with ablation electrode access or stability.

The number of lesions used to ablate each atrial septal zone significantly exceeded the postmortem lesion surface area. Several factors may account for this. First, we were very conservative in lesion spacing. Given that our goal was to pursue attenuation of interatrial conduction, minimizing the number of lesions was a secondary concern. This issue would obviously become more important in human trials employing this technique, during which mapping of right atrial activation during left atrial pacing may further enhance specificity and minimize the number of lesions required. Second, the areas reported herein were calculated from two-dimensional photographic planimetry. Given the complex topography of the right atrial septum, it is likely that this technique significantly underestimated the actual surface area. Finally, specimen shrinkage may have been a factor.

Study limitations. We emphasize several important limitations in our data. First, given the superior location of RAA and LAA electrodes, we cannot exclude the presence of significant changes in interatrial conduction changes after zone 2 ablation alone. Second, although we attributed increases in interatrial conduction time after right atrial septal ablation to trans-septal conduction delay, in this study, we did not map activation between RAA and LAA sites. Therefore, the site(s) of delay cannot be discerned with complete assurance. Third, AF inducibility in an unconditioned porcine model is poorly characterized and may not be predictive of the impact of the ablation procedure on previously reported AF in animal models or in humans. Finally, given that we performed no experiments to investigate the impact of the procedure duration or alternative site ablation on AF inducibility, it is possible that its relationship with septal ablation was coincidental. In this regard, the significant changes in SCL during the study indicate that variation in factors with potential influence on AF inducibility, such as autonomic tone, were likely to occur.

Reprint requests and correspondence: Dr. David Schwartzman, Cardiovascular Institute, Presbyterian University Hospital, B535, 200 Lothrop Street, Pittsburgh, Pennsylvania 15213-2582. E-mail: schwartzmand@msx.upmc.edu.

REFERENCES

1. Robb JS. The structure of the mammalian auricle. Womens Med J 1934;16:143–51.
2. Thomas CE. The muscular architecture of the atria of hog and dog hearts. Am J Anat 1959;104:207–36.
3. Papez JW. Heart musculature of the atria. Am J Anat 1920;27:255–85.
4. v Ludinghausen M, Ohmachi N, Boot C. Myocardial coverage of the coronary sinus and related veins. Clin Anat 1992;5:1–15.
5. Chauvin M, Shah DC, Haissaguerre M, et al. The anatomic basis of connections between the coronary sinus musculature and the left atrium in humans. Circulation 2000;101:647–52.
6. Inoue S, Becker AE. Posterior extensions of the human compact atrioventricular node: a neglected anatomic feature of potential clinical relevance. Circulation 1998;97:188–93.
7. Sanchez-Quintana D, Davies DW, Ho SY, et al. Architecture of the atrial musculature in and around the triangle of Koch: its potential relevance to atrioventricular nodal reentry. J Cardiovasc Electrophysiol 1997;8:1396–407.
8. James TN. The connecting pathways between the sinus node and A-V node and between the right and left atrium in the human heart. Am Heart J 1963;66:498–508.
9. Ho SY, Sanchez-Quintana D, Cabrera JA, et al. Anatomy of the left atrium: implications for radiofrequency ablation of atrial fibrillation. J Cardiovasc Electrophysiol 1999;10:1525–33.
10. Antz M, Otomo K, Arruda M, et al. Electrical conduction between the right atrium and the left atrium via the musculature in the coronary sinus. Circulation 1998;98:1790–5.
11. Sun H, Velipasaoglu EO, Wu DE, et al. Simultaneous multisite mapping of the right and left atrial septum in the canine intact beating heart. Circulation 1999;100:312–9.
12. Roithinger FX, Cheng J, SippensGroenewegen A, et al. Use of electroanatomic mapping to delineate transseptal atrial conduction in humans. Circulation 1999;100:1791–7.
13. Kumagai K, Khrestian C, Waldo AL. Simultaneous multisite mapping studies during induced atrial fibrillation in the sterile pericarditis model. Circulation 1997;95:511–21.
14. Allessie MA, Lammers WJEP, Bonke FIM, et al. Experimental evaluation of Moe's multiple wavelet hypothesis of atrial fibrillation. In: Zipes DP, Jalife J, editors. Cardiac Electrophysiology and Arrhythmias. Orlando, FL: Grune and Stratton, 1985:265–75.
15. Allessie M, Lammers W, Smeets J, et al. Total mapping of atrial excitation during acetylcholine-induced atrial flutter and fibrillation in the isolated canine heart. In: Kulbertus HE, Olsson SB, Schlepper M, editors. Atrial Fibrillation. Molndal, Sweden: Lindgren and Soner, 1982.
16. Skanes AC, Mandapati R, Berenfeld O, et al. Spatiotemporal periodicity during atrial fibrillation in the isolated sheep heart. Circulation 1998;98:1236–48.
17. Williams JM, Ungerleider RM, Lofland GK, et al. Left atrial isolation: new technique for the treatment of supraventricular arrhythmias. J Thorac Cardiovasc Surg 1980;80:373–80.
18. Ren J-F, Schwartzman D, Michele JJ, et al. Lower frequency (5 MHz) intracardiac echocardiography in a large swine model: imaging views and research applications. Ultrasound Med Biol 1997;23:871–7.
19. Schwartzman D, Kuck KH. Anatomy-guided linear atrial lesions for radiofrequency catheter ablation of atrial fibrillation. Pacing Clin Electrophysiol 1998;21:1959–78.
20. Ren JF, Schwartzman D, Callans DJ, et al. Intracardiac echocardiography (9 MHz) in humans: methods, imaging views and clinical utility. Ultrasound Med Biol 1999;25:1077–86.
21. Ren J-F, Schwartzman D, Callans DJ, et al. Imaging technique and clinical utility for electrophysiologic procedures of lower frequency (9 MHz) intracardiac echocardiography. Am J Cardiol 1998;82:1557–60.
22. Sueda T, Imai K, Nagata H, et al. Left atrial tachycardia after right atrial separation for chronic atrial fibrillation associated with atrial septal defects. Pacing Clin Electrophysiol 1999;22:1547–9.
23. van Hemel NM, Defauw JJ, Kingma JH, et al. Long-term results of the Corridor operation for atrial fibrillation. Br Heart J 1994;71:170–6.